UC Riverside

UC Riverside Electronic Theses and Dissertations

Title

Temporal Evolution of Heme Oxygenase-1 Expression in Reactive Astrocytes and Microglia Following Traumatic Brain Injury

Permalink

https://escholarship.org/uc/item/5dd6c5bf

Author

Morita, Alexander Shigekazu

Publication Date

2018

Copyright Information

UNIVERSITY OF CALIFORNIA
RIVERSIDE

Temporal Evolution of Heme Oxygenase-1 Expression in Activated Astrocytes and
Microglia Following Traumatic Brain Injury

A Thesis submitted in partial satisfaction
of the requirements for the degree of

Master of Science

in

Cell, Molecular, and Developmental Biology

by

Alexander Shigekazu Morita

December 2018

Thesis Committee:
    Dr. Andre Obenaus, Chairperson
    Dr. Martin Garcia-Castro
    Dr. Nicole zur Nieden

The Thesis of Alexander Shigekazu Morita is approved:

_____

_____

_____
                                                               Committee Chairperson

University of California, Riverside

Acknowledgements

Dedication

      I would like to dedicate this thesis to my family. I would also like to dedicate this to my friends Patrick Shelar and Carlos Rodriguez.

ABSTRACT OF THE THESIS

Temporal Evolution of Heme Oxygenase-1 Expression in Activated Astrocytes and
Microglia Following Traumatic Brain Injury

by

Alexander Shigekazu Morita

Master of Science, Graduate Program in Cell, Molecular, and Developmental Biology
University of California, Riverside, December 2018
Dr. Andre Obenaus, Chairperson

Heme oxygenase-1 (HO-1) is an inducible enzyme that catabolizes heme into biliverdin (which is converted to bilirubin), carbon monoxide, and free iron. Free iron, particularly Fe^{2+}, is known to have cytotoxic effects, via the Fenton reaction. Alternatively, bilirubin and carbon monoxide have antioxidant and anti-inflammatory functions, respectively, making the effects of HO-1 induction difficult to predict. In intracerebral hemorrhage, enhanced HO-1 expression has been reported to be beneficial. However, it is unknown if HO-1 expression has neuroprotective or neurodegenerative sequelae after traumatic brain injury (TBI). In our male mouse study, we quantitatively investigated HO-1 expression in reactive astrocytes and microglia in a controlled cortical impact (CCI) model of TBI at 1, 7, 14, and 30 days post-injury (dpi). Immunoglobulin G (IgG) staining as a measure of blood-brain barrier (BBB) permeability was significantly higher in 1 and 7dpi mice compared to controls, indicating BBB disruption early after TBI. HO-1 expression in astrocytes was significantly increased acutely and subacutely (1, 7, 14dpi) compared to controls.

In contrast, significantly elevated expression of HO-1 in microglia was only observed at chronic 14 and 30dpi time points relative to controls. This study demonstrates that HO-1 is highly expressed after TBI, but primarily in cells that contribute to the neuroinflammatory response and modulating this expression may provide a path to therapeutic intervention.

TABLE OF CONTENTS

List of Figures

Introduction

Traumatic brain injury (TBI) has been defined as a disruption in the normal functioning of the brain caused by a bump, blow, or jolt to the head, or penetrating head injury. It is estimated that there are 1.7 million people in the U.S. who are diagnosed with TBIs annually, and 275,000 of these individuals are hospitalized, and 52,000 result in death (Gardner and Zafonte, 2016). In terms of the temporal evolution of pathology, TBI has been described as being composed of two stages, primary and secondary injury. Primary injury occurs at the moment of impact and results from mechanical forces damaging cells in the brain. Neurons, glia, and blood vessels are damaged by these immediate mechanical forces which include acceleration/deceleration linear forces and rotational forces (McKee and Daneshvar, 2015).

TBI can also be classified as either focal or diffuse injury. Focal injury occurs more frequently in moderate and severe injury and involves contusions and mass lesion formation. Contusions involve mechanical disruption of neurons and glial cells, as well as vasculature which leads to blood-brain barrier disruption and/or hemorrhage. These events may lead to ischemia and induce necrosis within the core of the contusion. Upon neuronal necrosis, translocation of high-mobility group protein 1 (HMGB1) from the nucleus to the cytosol occurs. In the extracellular space, HMGB1 binds to tissue receptors which activate inflammatory cascades that cause more tissue damage, leading to expansion of the contusion (McGinn and Povlishock, 2015).

Diffuse neuronal or axonal injury can occur in mild, moderate, and severe injury. Mechanical forces can deform neuronal soma and dendritic membranes leading to temporary or persisting influx of various ions that are normally restricted to the extracellular environment. Milder forms of injury to the membrane may result in transient influx of ions and restoration of function of the membrane. However, severe injury may result in long-term disruption of membrane function and induction of neuronal cell death pathways. Diffuse axonal injury was originally described as a mechanical force tearing of axons. More recent studies involving anterograde tracers have shown that the shear forces and tensile loading result in impairment of axonal transport at single or multiple points along the axon (Stone et al., 2004). When impairment of axonal transport occurs, the axon cylinder swells which leads to disconnection of the axon (Povlishock et al., 1983). It has been presumed that axonal disconnection always results in neuronal death, but some studies have shown disconnection leads to enduring atrophic change and lays the groundwork for neuronal reorganization and axonal regeneration/repair (McGinn and Povlishock, 2015).

As mentioned earlier, primary injury results directly from the trauma and secondary injury results indirectly from the trauma. Primary injuries are a result of mechanical forces deforming brain tissue and disruption of normal functioning of the brain. Mechanical forces involved in brain injury include acceleration/deceleration linear forces, rotational forces, blunt impact, and penetration by projectile. These forces damage the neurons, axons, dendrites, glia, and blood vessels in focal or diffuse patterns (McKee and Daneshvar, 2015). Damage to the blood vessels results in intraparenchymal

2

hemorrhages, subdural hematomas (collection of blood in subdural space), and epidural hematomas (collection of blood between dura and skull) (Gardner and Zafonte, 2016).

Secondary injury involves processes that start seconds after injury and may be present decades later. Such processes include bleeding, excitotoxicity, calcium influx, and metabolic alterations (Hill et al., 2016). Vascular dysfunction following injury leads to ischemia due to impaired blood flow, formation of vasogenic edema, and loss of structural integrity of microvessels which leads to expansion of the hemorrhagic lesion (Kurland et al., 2012). Excitotoxicity involves excessive excitatory amino acid (glutamate/aspartate) signaling. A rapid and transient increase in extracellular glutamate occurs within minutes after TBI and comes from presynaptic nerve terminals of depolarized neurons and leakage from damaged neuronal and glial cells. A surge in glutamate stimulates glutamate receptors, which results in depolarization and excitotoxic damage which leads to necrosis in neurons and ionic dysregulation. Metabolic alterations arise from the increase in glutamate which initially increases glucose metabolism and is followed by a longer period of reduction in glycolysis (McGinn and Povlishock, 2015). Influx of calcium ions induces cellular damage through activation of calcium-dependent proteases, formation of reactive oxygen and nitrogen species, and impaired mitochondrial function (Xiong et al., 2013).

Heme oxygenases (HOs) are enzymes that degrade heme into carbon monoxide (CO), biliverdin, and ferrous iron (Fe^{2+}). Three isozymes (HO-1, HO-2, HO-3) are known and expressed in the endoplasmic reticulum. HO-1 is the inducible isoform and is expressed at high levels in the spleen and other tissues that degrade senescent

erythrocytes such as the liver and bone marrow (Ryter et al., 2006). HO-1 is also

expressed in the brain in microglia and neurons of the cerebellum, thalamus,

hypothalamus, cerebral cortex, and the hippocampal dentate gyrus (Schipper et al., 2009).

HO-2 is constitutively expressed and is expressed in various tissues such as the brain,

liver, kidney, gut and the testes (Ryter et al., 2006). In the brain, HO-2 is widely

distributed and mostly expressed in neurons, with the highest levels of expression in the

hippocampal pyramidal cells, dentate gyrus, and olfactory epithelium (Schipper et al.,

2009).

The breakdown products of heme oxygenase enzymatic activity have been shown

to have cytoprotective effects. While CO is known to be a known inhalation hazard, low

concentrations of CO have been shown to have cytoprotective functions. CO activates

soluble guanylyl cyclase which produces cGMP. When CO is applied to cells, it triggers

the proteolytic degradation of the proapoptotic p38α MAPK isoform which creates

favorable signaling for the antiapoptotic p38β MAPK isoform (Gozzelino et al., 2010).

Biliverdin can be converted to bilirubin by biliverdin reductase (BVR). Both biliverdin

and bilirubin have been shown to act as antioxidants for reactive oxygen species and

reactive nitrogen species (Ryter et al., 2006). Ferrous iron (Fe^{2+}) can bind to iron

regulatory proteins (IRPs), which influence the stability of mRNAs for proteins that

process and traffic iron such as ferritin. Once Fe^{2+} binds the IRP, it releases the IRP from

ferritin mRNA, allowing translation to occur. Ferritin scavenges free iron and can

accommodate iron up to about a 1:4,500 molar ratio. The bound iron is unavailable for

catalytic reactions until released (Ryter et al., 2006).

Heme oxygenase-1 was first shown to be expressed in the rat brain one day after fluid percussion model of traumatic brain injury. HO-1 expression was seen in the hippocampus and the deep cortical layer with an injury-dependent level of HO-1 expression seen in severe injury (Fukuda et al., 1995). In another fluid-percussion study on rats, induction of HO-1 was observed at 3- and 5-days post injury (dpi). There was a high degree of HO-1 expression in a zone surrounding the necrotic lesion in the cerebral cortex at 3dpi that decreased by 5dpi. HO-1 expression was seen in GFAP$^+$ cells near the necrotic lesion and OX42$^+$ cells further away from the lesion (Fukuda et al., 1996). In a cortical stab-wound injury study with rats, early HO-1 expression was minimal in neurons from 1-6 h post injury. Astrocyte expression of HO-1 started 12h after injury, peaked 3dpi, and declined by 5dpi to the point that they were rarely observed. HO-1$^+$/ED1$^+$cells were observed 1-3 dpi and were still present by 14dpi (Dwyer et al., 1996). ED1 is a lysosomal monocyte/macrophage antigen that is a marker for phagocytic microglia (Kullberg et al., 2001).

The function of HO-1 expression after neurological injury has been described in several studies to be neuroprotective. Cerebellar granular neurons isolated from mice overexpressing HO-1 in neurons had increased cell viability when exposed to glutamate or H_2O_2 mediated cell death (Chen et al., 2000). When the same strain of HO-1 overexpressing mice were subjected to middle cerebral artery occlusion (MCAO), they had decreased infarcts, decreased stroke volumes, and decreased ischemic cerebral edema (Panahian et al., 1999). The mechanism of HO-1 mediated neuroprotection in cultured

neuroblastoma cells was demonstrated through decreases in phosphorylated ERK-1 and ERK-2 and inhibition of HO-1 reversed this decrease (Chen et al., 2000).

More recent studies have shown the role of HO-1 as either neuroprotective or neurodegenerative, depending on the time after brain injury. In one study, HO-1 knockout mice had reduced injury volume, leukocyte infiltration, microglia/macrophage activation, and free radical levels 1 and 3 days after intracerebral hemorrhage (Wang and Dore, 2007). In another study with wild-type mice, increased HO-1 expression resulted in increased neurological deficits and injury volume 1 and 3 days after intracerebral hemorrhage (ICH). At 28 days after injury, inhibition of HO-1 resulted in more neurological deficits and increased hematoma volume, while stimulation of HO-1 expression resulted in increased angiogenesis (Zhang et al., 2017).

Studies have shown that overexpression of HO-1 in astrocytes may confer neuroprotection. Expression of human HO-1 in cultured astrocytes reduced cell death by 60% 1 day after hemin exposure (Benvenisti-Zarom and Regan, 2007). In a study with mice expressing human HO-1 in the astrocytes, there was reduced blood brain barrier damage and increased striatal cell viability following blood injection-induced ICH at early time points. These mice also appeared to perform better in neurological tests at early time points following ICH (Chen-Roetling et al., 2015). In a follow-up study with collagenase-induced ICH, the investigators also found increased neuron viability and decreased mortality in the transgenic mice compared to wild-type (Chen-Roetling et al., 2017).

In our study, we investigated HO-1 expression in activated astrocytes and microglia at various time points following controlled cortical impact (CCI) model of traumatic brain injury. Our study is novel since we investigated multiple time points and quantified the degree of HO-1 expression in reactive astrocytes and microglia at these time points. Based on previous studies, we hypothesize that HO-1 in glial cells modulates the hemorrhage and lesion after TBI and HO-1 expression in glial cells may lead to neuroprotection. The findings in this study provide insight into the evolution of HO-1 expression over time after traumatic brain injury and may lead further investigations into whether HO-1 could be a possible therapeutic target after TBI.

Materials and Methods

Animals

All animal experiments and care complied with federal regulations and were approved by the institutional animal health and safety committee. Adult male C57Bl/6J mice (N=26, 8-week-old, 25 g, Jackson laboratory, Bar Harbor, ME) were group-housed in cages on a 12-hour light-dark cycle at constant temperature and humidity. All animals were randomly assigned to five experimental groups: controls (N=4), TBI 1dpi (N=6), 7dpi (N=4), 14dpi (N=6), and 30dpi (N=6). A separate cohort was generated for tissue sections stained with IgG where male C57Bl/6J mice (N=13, 6-7-month-old, 20-30g, Jackson Laboratories) were randomly assigned to 2 groups: Sham or TBI. There were N=4 sham males, euthanized 1-day post-surgery. The TBI groups were euthanized 1dpi (N=4) or 7dpi (N=5).

Controlled Cortical Impact TBI Model

A CCI model of moderate brain injury was performed as previously described (Salehi et al., 2018). Briefly, mice were anesthetized (isoflurane 3% induction, 1.5% maintenance; Webster Veterinary Supply, Inc., Sterling, MA) and placed in a mouse stereotaxic frame (David Kopf Instruments, Tujunga, CA), with a heating pad that maintained body temperature at 37°C. Lidocaine (lidocaine hydrochloride 2%) was injected subcutaneously at the scalp incision site. A midline incision was performed to expose the skull surface of anesthetized mice and a 5 mm craniotomy was performed, centered 2.5 mm posterior and 2.5 mm lateral from Bregma on the right side.

A moderate CCI (3 mm diameter tip, 1.5 mm depth, 2.0 m/s speed, 200 ms dwell) was delivered to the cortical surface using an electromagnetically driven piston (Leica Microsystems Company, Richmond, IL). The skin was sutured and Buprenorphine (0.01 mg/kg, intramuscular) was administered after surgery to minimize pain. Control animals were anesthetized for the identical period of time as injury animals and administered buprenorphine. Injured animals were randomly selected and euthanized at the selected time points (1, 7, 14, 30 days). Control animals (only administered isoflurane and buprenorphine) were euthanized at 3 days after exposure. Sham animals went under the same procedure as injured animals but without cortical impact and were euthanized 1-day post-surgery.

<div align="center">Immunohistochemistry</div>

Animals were sacrificed by transcardial perfusion with phosphate buffered saline (PBS) and 4% paraformaldehyde (PFA). Prior to cryosectioning brains were placed in 30% sucrose and embedded in optimal cutting temperature compound (O.C.T. Compound, #4583, Tissue Tek; Sakura Fine Tek, Torrance, CA). 25 μm-thick coronal sections were cut using a Leica CM1850 cryostat (Leica Microsystems GmbH, Wetzlar Germany), mounted directly on microscope slides (Fisherbrand^{TM} Superfrost Plus Microscope Slides, #12-550-15, Fisher Scientific, Pittsburgh, PA) and kept at -20°C.

Mounted sections were labeled with anti-rabbit HO-1 (1:200, Enzo Life Sciences Cat# ADI-SPA-895, Farmingdale, NY, RRID: AB_10618757), incubated in PBS+0.5% bovine serum albumin (BSA) at room temperature overnight.

Sections were simultaneously labeled with either anti-mouse glial fibrillary acidic protein (GFAP; 1:500, EMD Millipore Cat#MAB3402, Burlington, MA, RRID: AB_94844) or anti-goat allograft inflammatory factor 1 (AIF-1)/ionized calcium-binding adapter molecule 1 (Iba1; 1:200, Novus Biologicals Cat#NB100-1028, Littleton, CO, RRID: AB_521594), or anti-mouse neuronal-specific nuclear protein (NeuN; 1:800, EMD Millipore Cat#MAB377, Burlington, MA, RRID: AB_2298772) at room temperature overnight. Sections were then incubated with goat anti-rabbit Alexa Fluor® 594 (1:1000, Thermo Fisher Cat #A-11012, Waltham, MA, RRID: AB_2534079), donkey anti-rabbit Alexa Fluor® 594 (1:1000, Thermofisher Cat#A-21207, RRID: AB_141637) and goat anti-mouse Alexa Fluor® 488 (1:1000, Thermo Fisher Cat#A-11029, RRID: AB_2534088) or donkey anti-goat Alexa Fluor® 488 (1:1000, Thermo Fisher Cat#A-11055, RRID: AB_2534102) for 1.5 hours. For IgG staining, sections were incubated with anti-mouse IgG-fluorescein isothiocyanate (FITC) antibody (1:200, Sigma-Aldrich #F0257, city, state, RRID: AB_259378) at room temperature overnight. Sections were coverslipped by using Vectashield HardSet Antifade Mounting Medium with DAPI (Vector Laboratories #H-1500, Burlingame, CA, RRID: AB_2336788).

Microscopy

A BZ-X700 Keyence microscope (Keyence Corp, Elmwood Park, NJ) was used to acquire the images using Z-stacks of the coronal sections using 1 μm steps encompassing 25 slices and resulting in a 25 μm slab. Following acquisition, BZ-II Analyzer software (Keyence Corp, Elmwood Park, NJ, RRID: SCR_016348) was used to merge Z-stacks into full focus images.

Image processing included adjustment of brightness and contrast for each of the acquired images. 2x images of the whole brain slice were obtained by using XY-stitching. Image correction using black balance was performed only for tissue stained with the anti-IgG antibody.

<center>Histological Measurements</center>

In order to determine tissue loss as a result of TBI, 2x images were acquired to measure the brain area on both right and left hemispheres. Using ImageJ software (National Institutes of Health, Rockville, MD, RRID: SCR_003070), regions of interest (ROI) for both right and left hemispheres were drawn by a blinded experimenter (Figure 1A). Areas were measured to compare the difference between the ipsilateral and contralateral hemispheres to obtain a ratio (ipsilateral area: contralateral area) where a decreased ratio would denote TBI severity.

To evaluate BBB disruption, IgG images (2x) were analyzed by a blinded experimenter using ImageJ software, where integrated density measurements were performed on the top right quarter of the brain that contained the lesion site (Figure 3A).

<center>Quantification of Cell Counts</center>

Two 20x images of the cortex (Figure 1B) adjacent to the lesion (-1.70 to -1.90 mm relative to Bregma) were analyzed independently by 2 blinded experimenters using Image-Pro Premier software (v9.1, Media Cybernetics, Rockville, MD, RRID: SCR_016497). The brightness of the color channels (red for HO-1, green for GFAP or Iba-1) were minimized to remove background and values of the brightness were recorded.

A colocalization mask of the red and green colocalized pixels was used to create a composite image with the blue channel for DAPI staining. Thresholds for the red and green color channels were normalized to the recorded brightness measurements. To determine the number of astrocytes (GFAP+) or microglial cells (Iba1+) stained with HO-1, DAPI+ cells containing colocalized pixels were counted by manual tagging. DAPI+ cells with less than 75% overlap with the colocalized pixels were not counted. Cell counts from the two images were then averaged to a single value. The personnel conducting the cell counts were blinded to the treatment conditions.

<div align="center">Statistics</div>

One-way analysis of variance (ANOVA), Tukey's multiple comparisons tests were performed using GraphPad (GraphPad Prism 7.0, San Diego, CA, RRID: SCR_002798). The data for the parametric tests exhibited a normal distribution and passed the Shapiro-Wilk normality tests. Values are presented as mean ± SEM with statistical significance reported at *=$p<0.05$, **=$p<0.01$, ***=$p<0.001$ and ****=$p<0.0001$. Outliers were removed if they were above or below 1.5 times the interquartile range (IQR).

Results

All animals survived the TBI procedure and there were significant differences in body weight in animals over the time course before surgery to 30dpi. There was no significant difference in weights before surgery and 1dpi (Paired t-test, p=0.46) and 7dpi (Paired t-test, p=0.20). There was a significant difference in weights in animals before surgery and 14dpi (Paired t-test, p=0.05) and 30dpi (Paired-test, p<0.01). There was no significant difference seen in control animals that were only administered with isoflurane and sacrificed 3 days later (Paired t-test, p=.34).

Tissue Loss and BBB Disruption and total HO-1$^+$ cell counts

To characterize the relationship with TBI and HO-1, we assessed tissue loss and BBB disruption as well as the total counts of HO-1$^+$ cells after TBI, using ImageJ to measure ipsilateral and contralateral area and IgG staining of brain tissue. In the ipsilateral hemisphere was significant tissue loss at 30dpi (87.24±0.02% remaining) compared to control mice (97.94±0.01% remaining; p=0.013; Figure 1C). At 1dpi, cells expressing HO-1 appeared to be primarily astrocytes and microglia, but not neurons (Figure 2A-C). The number of HO-1$^+$ cells (colocalized only with DAPI) was significantly higher between 7dpi (311.60±51.02 cells; p=0.03) and 14dpi (298.20±30.63 cells; p=0.03) vs control (91.50±41.04 cells). There was no significant difference between 1dpi (275.00±45.54 cells; p=0.06), 30dpi (239.20±43.93 cells; p=.21) and control (91.50±41.04 cells) (Figure 2D).

Evaluation of BBB integrity using IgG staining showed an increased permeability at 1dpi that was resolved by 7dpi (Figure 3B-E). BBB quantification in the injured hemisphere revealed significantly increased staining density in 1dpi (803.83±147.47 p=0.001) and 7dpi mice (679.60±337.27; p=0.0043) compared to sham controls (136.49±55.38; Figure 3F). BBB disruption was significantly reduced at 14dpi (211.87±82.23; p=0.004), and 30dpi (49.84±9.45; p=0.0004) compared to 1dpi. There was also a significant decrease between 7dpi and 30dpi (p=0.002; Figure 3F). The BBB in our model of TBI is disrupted at 1-7dpi but this perturbation appeared to recover to control levels by 14 and 30dpi.

<div align="center">HO-1 Colocalization in Astrocytes</div>

Immunostaining for HO-1 and GFAP at 1, 7, 14, and 30dpi revealed significant increases in HO-1 and GFAP colocalization (Figure 4A-E). The expression of HO-1$^+$ astrocytes appears in a sub-population of astrocytes as not all GFAP$^+$ cells express HO-1. Compared to control mice (1.75±0.47 cells), significant increases in the number of astrocytes co-localizing HO-1 at 1dpi (35.33±6.25 cells; p=0.006), 7dpi (47.50±3.52 cells; p<0.0001), and 14dpi (33.60±4.88 cells; p=0.002) were observed. The number of HO-1/GFAP colocalized cells significantly decreased from 7dpi (47.50±3.52 cells) to 30dpi (22.50±2.53 cells; p=0.02; Figure 4F). It is apparent at certain time points that not all the astrocytes express HO-1, as evidenced by the lack of HO-1 staining in some GFAP$^+$ cells (Figures 4C-4D).

HO-1 Colocalization in Microglia

Immunostaining for HO-1 and Iba1 over the same time course also displayed a robust

increase in HO-1 and Iba1 colocalization (Figure 5A-E). There was a significant increase

in HO-1$^+$ cells between controls (25.5±9.53 cells) and 14dpi (228.33±29.55 cells;

p=0.001) and 30dpi (147.33±36.25 cells; p=0.0245). There was also a significant increase

in HO-1$^+$ microglial cells between 1dpi (57.14±5.78 cells) and 14dpi (228.33±29.55 cells;

p=0.0002), 7dpi (103.6±19.93 cells) and 14dpi (228.33±29.55 cells; p=0.0124; Figure

5F).

Comparisons of HO-1 Colocalization in Astrocytes and Microglia

In examining the temporal evolution of HO-1+cells between astrocytes and

microglia it was clear that there were a higher number of microglia cells expressing HO-

1, particularly at the later time points. Comparing the number of HO-1$^+$ astrocytes and

HO-1$^+$ microglia across all time points, we found significantly increased numbers of HO-

1$^+$ microglia (228.33±29.55) at 14dpi compared to HO-1$^+$ astrocytes at the same time

point (33.60±4.88 cells; p<0.0001). The same holds for 30dpi, where there were

significantly increased numbers of HO-1$^+$ microglia (147.33±36.25 cells) relative to HO-

1$^+$ astrocytes (22.50±2.53 cells; p<0.0001).

Morphological Comparisons of HO-1 Colocalization in Astrocytes and Microglia

Astrocyte morphology is altered in mild to severe reactive astrogliosis (Sofroniew

and Vinters, 2010). In severe injury, diffuse reactive astrogliosis results in pronounced

hypertrophy of cell body and processes with crossing of neighboring astrocyte processes

resulting in blurring and disruption of individual astrocyte domains (Sofroniew and

Vinters, 2010). Some astrocytes expressing HO-1 at 1dpi appeared to be of the reactive

subtype (Figure 6A). At 7dpi the astrocytes that colocalized HO-1 possessed thicker

processes extending from more pronounced hypertrophic cell bodies which were still

observed at 14dpi (Figure 6A). In microglia, HO-1 expression was found in round-shaped

microglia with long processes at 1dpi (Figure 6B) but by 7dpi HO-1$^+$ microglia appeared

to be swollen with contracted processes, indicative of an ameboid morphology (Figure

6B).

<center>Temporal Aspects of HO-1 Expression</center>

Comparison of the temporal evolution of HO-1$^+$ astrocytes and microglia

demonstrated that HO-1$^+$ microglia peaked at 14dpi while astrocytic numbers were

maximal at 7dpi, with 27-fold increase above controls (Figure 7A). The number of HO-1$^+$

astrocytes was reduced by 14dpi but did not return to control levels by 30dpi, where it

remained elevated 13-fold more than controls. The number of microglia expressing HO-1

reached a 9-fold peak over controls at 14dpi was still elevated and remained 6-fold over

controls. This novel finding would suggest a sustained level of HO-1 expression in

inflammatory microglial cells in perilesional tissues even at chronic periods after TBI.

The percentage contribution of HO-1 expression in GFAP$^+$ or Iba1$^+$ to total HO-

1$^+$ cells was determined. The estimated percentage of HO-1$^+$ GFAP$^+$ cells out of the total

number of HO-1$^+$ cells in the injury groups ranges from 10.53% (30dpi) to a maximum of

22.22% at 7dpi (Figure 7B). The estimated percentage of HO-1$^+$ Iba1$^+$ cells out of the

total number of HO-1$^+$ cells in the injury groups ranged from 20.78% (1dpi) to a

maximum of 76.56% at 14dpi (Figure 7B).

<center>16</center>

Discussion

HO-1 expression is increased in numerous acquired neurological injuries. In TBI there have been no reports of the quantitative distribution of HO-1+ glial cells. While astrocytes and microglia are glial cells, they are distinct cells and express different levels of HO-1 over time. Astrocytes are derived from neural stem cells, which also give rise to neurons (Alvarez-Buylla et al., 2001) . Microglia are derived from yolk sac macrophages that seed the brain during early development, and embryonic microglia grow and span the entire CNS until adulthood (Ginhoux et al., 2013). We describe for the first time the temporal evolution of perilesional HO-1 expression in reactive astrocytes and microglia following a moderate TBI injury in male mice. We did not observe HO-1 in neurons, suggesting that it is not induced in this cellular population in response to TBI . We observed a high level of HO-1 expression in microglia that peaked at 14dpi, but which remained elevated at 30dpi compared to control levels. Astrocytic HO-1 expression was significantly lower than that of microglia, following a more gradual pattern peaking at 7dpi, and decreasing by 30dpi. Notably, the HO-1 response in both astrocytes and microglia was still elevated (relative to controls) at 30dpi consistent with the hypothesis of ongoing inflammation. Our novel study is the first to quantitatively and temporally examine HO-1 in glial cells over the course of 30 days following TBI.

Our observation of virtually no HO-1 expression in neurons in our study and predominately in astrocytes and microglia is consistent with a previous study where Chang and colleagues performed CCI in HO-2 knockout mice (Chang et al., 2003).

They found that HO-2 was detected in the neurons throughout the brain but HO-1 was detected only in glial cells. Other studies have on occasion described minimal HO-1 expression in neurons but not contributing greatly to overall HO activity after Liu and colleagues found HO-1 expression in neurons in the ipsilateral cortex after weight-drop induced-TBI in rats, but this level of expression was not significantly different compared to the contralateral cortex (Liu et al., 2013). These findings including our own, would suggest that HO-1 expression is restricted to glial cells. However, neuronal expression of HO-1 has been in reported in primary cultures of ventral mesencephalon neurons after treatment with oxidative stress inducer mitochondria complex 1-methyl-4-phenylpyridinium. However, the authors of that study note HO-1 expression was induced earlier in cultured astrocytes, hinting that it might be more efficiently expressed in those cells than in neurons (Yu et al., 2016).

HO-1 expression in the developing rat brain has been shown to change over time with widespread expression in multiple regions of the brain in P7 rats and intense in regions of myelinogenesis of white matter (Bergeron et al., 1998). In adult rats, the expression profile was intense in areas such as hypothalamus and the dentate gyrus. HO-1 was detected in microglia-like cells and neurons in the cortex which decreased with age (Bergeron et al., 1998). In our study we did not detect overt HO-1 staining in the cortex of uninjured animals (Figures 4A, 5A). The expression of HO-1 in its role in neonatal or juvenile TBI has not been studied. Future work should investigate if there is a difference in HO-1 expression in younger animals after TBI, and a potential area of interest could be myelin, which has been shown to be modified after juvenile TBI (Lee, 2018).

Previous work has shown that myelin basic protein induces expression of HO-1 in human astroglial cells (Businaro et al., 2002).

The predominant expression of HO-1 in microglia is similar to those observed by Liu and colleagues (Liu et al., 2013) in a rat open-skull weight-drop induced-TBI model. They detected HO-1^{+} microglia in the cortex as early as 18h post-injury and up through 96h post-injury and these were significantly higher than in controls. While we observed HO-1^{+} microglia at 1dpi the numbers of microglia expressing HO-1 did reach significance until 14dpi. However, surprisingly in contrast to our findings, Liu and colleagues did not detect GFAP[+] HO-1^{+} cells. We found that HO-1^{+} astrocytes were observed early but in general HO-1 was expressed mostly in microglia following moderate TBI. HO-1 expression in microglia at 3 days after a fluid percussion injury in rats has been reported, but in this model of brain injury it appears that HO-1 is mainly expressed in astrocytes (Fukuda et al., 1996) and confirmed in a lateral fluid percussion injury (Yi and Hazell, 2005). Differences between TBI models highlight contrasting mechanisms of HO-1 expression and the level of subsequent inflammation. As, such, the model of injury should be taken into consideration when interpreting outcomes.

HO-1 expression in microglia has also been reported in other types of brain injury. Hyperosmotic opening of the BBB induced expression of HO-1 in astrocytes and microglia (Richmon et al., 1998). HO-1 expression in microglia/macrophages was detected 24h after collagenase-induced intracerebral hemorrhage in mice (Wang and Dore, 2007). These studies suggest that the function of microglial HO-1 after brain hemorrhage may act to prevent neuronal death.

19

A previous study by Schallner and colleagues demonstrated that deletion of HO-1 in microglia reduced erythrophagocytosis and increased neuronal apoptosis after subarachnoid hemorrhage (Schallner et al., 2015). Thus, hemorrhagic events as a result of TBI would suggest that HO-1 may have a similar function as that reported in intracerebral/subarachnoid hemorrhage, but additional studies need to be undertaken to definitively evaluate the role of HO-1$^+$ microglia after TBI.

In contrast to the late expression of microglia, we found that astrocytes expressed HO-1 as early as 1dpi and continued through 30dpi. In a cortical stab wound model HO-1$^+$ astrocytes were observed as early as 12h post-injury that declined by 3d near the wound area in rats (Dwyer et al., 1996). HO-1$^+$ astrocytes have also been observed after fluid percussion TBI (Fukuda et al., 1996). Recently, we reported sex differences in HO-1 expression in TBI where increased HO-1 expression and increased astrocyte reactivity were observed in the injured cortex in females at 1dpi but not males(Jullienne et al., 2018; Jullienne, 2018)). Curiously, HO-1$^+$ astrocytes were not observed after weight drop injury in rats but this may reflect the relative severity of the injury (Liu et al., 2013). It is clear that the role of increased HO-1 expression in astrocytes remains to be clarified in TBI.

An interesting observation of our study was the time to peak HO-1$^+$ expression in astrocytes (7dpi) and in microglia (14dpi). Other CCI TBI studies have found peak expression of GFAP and OX-42 (a microglia/macrophage marker) at 4dpi (Chen et al., 2003) and in C57BL/6 mice astrogliosis peaked at 3dpi (Villapol et al., 2014). These findings in combination with our results, would suggest that the level of HO-1 expression

does not necessarily need coincide with peak astrocyte or microglia activation in the injured cortex. Villapol and colleagues noted that the peak level of apoptosis in the perilesional cortex was 5 hours post-injury and this high level persisted through 3dpi (Villapol et al., 2014). A cell culture study on mouse neurons overexpressing HO-1 found that increased levels of HO-1 resulted in decreased cell death when exposed to glutamate (Chen et al., 2000). The physiological significance of the temporal HO-1+ expression patterns in astrocytes and microglia requires future study, particularly as it relates to the known inflammatory responses of these cells in TBI.

It is important to note that not all the HO-1$^+$ cells expressed either GFAP or Iba1. The total number of colocalized cells (HO-1/GFAP, HO-1/Iba1) only contributed to about 30% of the cells for the control animals, 33% of the total HO-1+ cells at the 1d time point, and about 49% at the 7d time point (Figure 7B). The percentage did increase to about 87% at the 14d time point and 70% at the 30d time point. GFAP is a marker for reactive astrocytes, but it has been shown that many mature astrocytes in healthy CNS tissue do not express detectable levels of GFAP (Sofroniew and Vinters, 2010). Other potential astrocyte markers could include S100B or ALDHL1. S100B has been described to be expressed in astrocytes, but has been shown in studies not to be astrocyte-specific, staining oligodendrocytes and lymphocytes (Steiner et al., 2007). Aldehyde dehydrogenase 1 family, member L1 (ALDHL1), has been described as an astrocyte specific marker, and has been shown to label more astrocytes than GFAP staining(Cahoy et al., 2008). If additional astrocytes could be identified with either of these markers, it is possible some of these cells may also be expressing HO-1.

Also, endothelial cells are another cell type that could express HO-1 after TBI, as reported in cultured cerebral microvascular endothelial cells (Parfenova et al., 2006) and endothelial cells after middle cerebral artery occlusion (Nimura et al., 1996).

Differences in TBI models and injury severity may underlie some of the reported differences between studies. In contrast to our own findings wherein we observed increased GFAP staining as early as 1dpi (Figure 2B), Villapol and colleagues did not observe any signs of astrogliosis at early time points following a milder form of TBI (Villapol et al., 2014). Chen and colleagues were able to detect expression of GFAP as early as 1dpi using severe CCI model in rats (Chen et al., 2003). In our model of moderate TBI, at 7dpi we observed robust HO-1 expression in a subset of astrocytes (Figure 3C) with diminution over 30dpi, but with HO-1$^+$ astrocytes present at latter time points (Figures 3D-E, 6A). In our study, the elevation in HO-1$^+$ astrocytes and microglia appeared to be limited to the region around the necrotic lesion, similar to that of fluid percussion injury (Fukuda et al., 1996).

There have been few studies examining regulators of HO-1 expression after TBI. Park and colleagues found that Toll-like receptor 2 (TLR2) is necessary for glial cell activation and HO-1 expression in the stab wound injured mouse brain (Park et al., 2008). TLR2 knockout mice exhibited reduced HO-1 expression after injury as well as decreased astrocyte and microglia activation, suggesting TLR2 may be a mediator of glial activation and HO-1 expression after TBI. Expression of TLR2, TLR4, MyD88 and HSP70 were detected after an open-skull weight drop injury (Zhang et al., 2012). Toll-like receptor signaling was also investigated after CCI by Krieg and colleagues.

They knocked out TLR2 and TLR4, and discovered decreased contusion volume, increases in IL-1β, and decreased IL-6 and HMGB1 in the knockout mice compared to WT controls at early time points (Krieg et al., 2017). It would appear modulation of TLR signaling may be important in modulating HO-1 expression and inflammation, but more long-term studies need to be done to establish a clear role in this signaling pathway after TBI.

There have been few studies investigating long-term expression of HO-1 after TBI. The first long-term study was done with human tissue, where HO-1 expression was prevalent as late as 6 months post injury (Beschorner et al., 2000). Our results show that HO-1 is still expressed in astrocytes and microglia up to 30 days after CCI, which is in agreement with Chang and colleagues, where they detected HO-1 in microglia and astrocytes in areas next to the area of impact after using CCI in mice by 14dpi (Chang et al., 2003). The long-term presence of HO-1 in the brain after TBI should be investigated since secondary injury mechanisms play a significant role in long-term outcomes.

In conclusion, temporal HO-1 expression differs dramatically between astrocytes and microglia after TBI, highlighting the need to carefully assess these primary inflammatory cells. Both HO-1$^+$ microglia and HO-1$^+$ astrocytes are observed to be at expression levels early TBI but as the injury matures there are significantly higher levels of HO-1$^+$ microglia by 14 and 30dpi. The maintained HO-1 expression in inflammatory cells may contribute to minimizing known microglial oxidative stress as well as potentially limiting lesion expansion in response to cortical tissue injury in TBI.

It remains to be determined if enhancing HO-1 expression in reactive astrocytes and microglia can promote an earlier and sustained morphological and functional recovery after TBI.

References

Alvarez-Buylla, A., J.M. Garcia-Verdugo, and A.D. Tramontin. 2001. A unified hypothesis on the lineage of neural stem cells. *Nature reviews. Neuroscience.* 2:287-293.

Benvenisti-Zarom, L., and R.F. Regan. 2007. Astrocyte-specific heme oxygenase-1 hyperexpression attenuates heme-mediated oxidative injury. *Neurobiology of disease.* 26:688-695.

Bergeron, M., D.M. Ferriero, and F.R. Sharp. 1998. Developmental expression of heme oxygenase-1 (HSP32) in rat brain: an immunocytochemical study. *Brain research. Developmental brain research.* 105:181-194.

Beschorner, R., D. Adjodah, J.M. Schwab, M. Mittelbronn, I. Pedal, R. Mattern, H.J. Schluesener, and R. Meyermann. 2000. Long-term expression of heme oxygenase-1 (HO-1, HSP-32) following focal cerebral infarctions and traumatic brain injury in humans. *Acta neuropathologica.* 100:377-384.

Businaro, R., C. Fabrizi, B. Caronti, C. Calderaro, L. Fumagalli, and G.M. Lauro. 2002. Myelin basic protein induces heme oxygenase-1 in human astroglial cells. *Glia.* 37:83-88.

Cahoy, J.D., B. Emery, A. Kaushal, L.C. Foo, J.L. Zamanian, K.S. Christopherson, Y. Xing, J.L. Lubischer, P.A. Krieg, S.A. Krupenko, W.J. Thompson, and B.A. Barres. 2008. A transcriptome database for astrocytes, neurons, and oligodendrocytes: a new resource for understanding brain development and function. *The Journal of neuroscience : the official journal of the Society for Neuroscience.* 28:264-278.

Chang, E.F., R.J. Wong, H.J. Vreman, T. Igarashi, E. Galo, F.R. Sharp, D.K. Stevenson, and L.J. Noble-Haeusslein. 2003. Heme oxygenase-2 protects against lipid peroxidation-mediated cell loss and impaired motor recovery after traumatic brain injury. *The Journal of neuroscience : the official journal of the Society for Neuroscience.* 23:3689-3696.

Chen-Roetling, J., P. Kamalapathy, Y. Cao, W. Song, H.M. Schipper, and R.F. Regan. 2017. Astrocyte heme oxygenase-1 reduces mortality and improves outcome after collagenase-induced intracerebral hemorrhage. *Neurobiology of disease.* 102:140-146.

Chen-Roetling, J., W. Song, H.M. Schipper, C.S. Regan, and R.F. Regan. 2015. Astrocyte overexpression of heme oxygenase-1 improves outcome after intracerebral hemorrhage. *Stroke.* 46:1093-1098.

Chen, K., K. Gunter, and M.D. Maines. 2000. Neurons overexpressing heme oxygenase-1 resist oxidative stress-mediated cell death. *Journal of neurochemistry.* 75:304-313.

Chen, S., J.D. Pickard, and N.G. Harris. 2003. Time course of cellular pathology after controlled cortical impact injury. *Experimental neurology.* 182:87-102.

Dwyer, B.E., R.N. Nishimura, S.Y. Lu, and A. Alcaraz. 1996. Transient induction of heme oxygenase after cortical stab wound injury. *Brain research. Molecular brain research.* 38:251-259.

Fukuda, K., S.S. Panter, F.R. Sharp, and L.J. Noble. 1995. Induction of heme oxygenase-1 (HO-1) after traumatic brain injury in the rat. *Neuroscience letters*. 199:127-130.

Fukuda, K., J.D. Richmon, M. Sato, F.R. Sharp, S.S. Panter, and L.J. Noble. 1996. Induction of heme oxygenase-1 (HO-1) in glia after traumatic brain injury. *Brain research*. 736:68-75.

Gardner, A.J., and R. Zafonte. 2016. Neuroepidemiology of traumatic brain injury. *Handb Clin Neurol*. 138:207-223.

Ginhoux, F., S. Lim, G. Hoeffel, D. Low, and T. Huber. 2013. Origin and differentiation of microglia. *Front Cell Neurosci*. 7:45.

Gozzelino, R., V. Jeney, and M.P. Soares. 2010. Mechanisms of cell protection by heme oxygenase-1. *Annual review of pharmacology and toxicology*. 50:323-354.

Hill, C.S., M.P. Coleman, and D.K. Menon. 2016. Traumatic Axonal Injury: Mechanisms and Translational Opportunities. *Trends in neurosciences*. 39:311-324.

Jullienne, A., A. Salehi, B. Affeldt, M. Baghchechi, E. Haddad, A. Avitua, M. Walsworth, I. Enjalric, M. Hamer, S. Bhakta, J. Tang, J.H. Zhang, W.J. Pearce, and A. Obenaus. 2018. Male and Female Mice Exhibit Divergent Responses of the Cortical Vasculature to Traumatic Brain Injury. *Journal of neurotrauma*. 35:1646-1658.

Krieg, S.M., F. Voigt, P. Knuefermann, C.J. Kirschning, N. Plesnila, and F. Ringel. 2017. Decreased Secondary Lesion Growth and Attenuated Immune Response after Traumatic Brain Injury in Tlr2/4(-/-) Mice. *Frontiers in neurology*. 8:455.

Kullberg, S., H. Aldskogius, and B. Ulfhake. 2001. Microglial activation, emergence of ED1-expressing cells and clusterin upregulation in the aging rat CNS, with special reference to the spinal cord. *Brain research*. 899:169-186.

Kurland, D., C. Hong, B. Aarabi, V. Gerzanich, and J.M. Simard. 2012. Hemorrhagic progression of a contusion after traumatic brain injury: a review. *J Neurotrauma*. 29:19-31.

Lee, J.B., Affeldt, B.M., Gamboa, Y., Hamer, M., Dunn, J.F., Pardon, A.C., Obenaus, A. 2018. Repeated Pediatric Concussions Evoke Long-Term Oligodendrocyte and White Matter Microstructural Dysregulation Distant from the Injury. U.o.C. Department of Pediatrics, Irvine, editor, Developmental Neuroscience.

Liu, Y., Z. Zhang, B. Luo, H.J. Schluesener, and Z. Zhang. 2013. Lesional accumulation of heme oxygenase-1+ microglia/macrophages in rat traumatic brain injury. *Neuroreport*. 24:281-286.

McGinn, M.J., and J.T. Povlishock. 2015. Cellular and molecular mechanisms of injury and spontaneous recovery. *Handb Clin Neurol*. 127:67-87.

McKee, A.C., and D.H. Daneshvar. 2015. The neuropathology of traumatic brain injury. *Handb Clin Neurol*. 127:45-66.

Nimura, T., P.R. Weinstein, S.M. Massa, S. Panter, and F.R. Sharp. 1996. Heme oxygenase-1 (HO-1) protein induction in rat brain following focal ischemia. *Brain research. Molecular brain research*. 37:201-208.

Panahian, N., M. Yoshiura, and M.D. Maines. 1999. Overexpression of heme oxygenase-1 is neuroprotective in a model of permanent middle cerebral artery occlusion in transgenic mice. *Journal of neurochemistry*. 72:1187-1203.

Parfenova, H., S. Basuroy, S. Bhattacharya, D. Tcheranova, Y. Qu, R.F. Regan, and C.W. Leffler. 2006. Glutamate induces oxidative stress and apoptosis in cerebral vascular endothelial cells: contributions of HO-1 and HO-2 to cytoprotection. *American journal of physiology. Cell physiology*. 290:C1399-1410.

Park, C., I.H. Cho, D. Kim, E.K. Jo, S.Y. Choi, S.B. Oh, K. Park, J.S. Kim, and S.J. Lee. 2008. Toll-like receptor 2 contributes to glial cell activation and heme oxygenase-1 expression in traumatic brain injury. *Neuroscience letters*. 431:123-128.

Povlishock, J.T., D.P. Becker, C.L. Cheng, and G.W. Vaughan. 1983. Axonal change in minor head injury. *Journal of neuropathology and experimental neurology*. 42:225-242.

Richmon, J.D., K. Fukuda, N. Maida, M. Sato, M. Bergeron, F.R. Sharp, S.S. Panter, and L.J. Noble. 1998. Induction of heme oxygenase-1 after hyperosmotic opening of the blood-brain barrier. *Brain research*. 780:108-118.

Ryter, S.W., J. Alam, and A.M. Choi. 2006. Heme oxygenase-1/carbon monoxide: from basic science to therapeutic applications. *Physiological reviews*. 86:583-650.

Salehi, A., A. Jullienne, M. Baghchechi, M. Hamer, M. Walsworth, V. Donovan, J. Tang, J.H. Zhang, W.J. Pearce, and A. Obenaus. 2018. Up-regulation of Wnt/beta-catenin expression is accompanied with vascular repair after traumatic brain injury. *Journal of cerebral blood flow and metabolism : official journal of the International Society of Cerebral Blood Flow and Metabolism*. 38:274-289.

Schallner, N., R. Pandit, R. LeBlanc, 3rd, A.J. Thomas, C.S. Ogilvy, B.S. Zuckerbraun, D. Gallo, L.E. Otterbein, and K.A. Hanafy. 2015. Microglia regulate blood clearance in subarachnoid hemorrhage by heme oxygenase-1. *The Journal of clinical investigation*. 125:2609-2625.

Schipper, H.M., W. Song, H. Zukor, J.R. Hascalovici, and D. Zeligman. 2009. Heme oxygenase-1 and neurodegeneration: expanding frontiers of engagement. *Journal of neurochemistry*. 110:469-485.

Sofroniew, M.V., and H.V. Vinters. 2010. Astrocytes: biology and pathology. *Acta neuropathologica*. 119:7-35.

Steiner, J., H.G. Bernstein, H. Bielau, A. Berndt, R. Brisch, C. Mawrin, G. Keilhoff, and B. Bogerts. 2007. Evidence for a wide extra-astrocytic distribution of S100B in human brain. *BMC Neurosci*. 8:2.

Stone, J.R., D.O. Okonkwo, A.O. Dialo, D.G. Rubin, L.K. Mutlu, J.T. Povlishock, and G.A. Helm. 2004. Impaired axonal transport and altered axolemmal permeability occur in distinct populations of damaged axons following traumatic brain injury. *Experimental neurology*. 190:59-69.

Villapol, S., K.R. Byrnes, and A.J. Symes. 2014. Temporal dynamics of cerebral blood flow, cortical damage, apoptosis, astrocyte-vasculature interaction and astrogliosis in the pericontusional region after traumatic brain injury. *Frontiers in neurology*. 5:82.

Wang, J., and S. Dore. 2007. Heme oxygenase-1 exacerbates early brain injury after intracerebral haemorrhage. *Brain : a journal of neurology*. 130:1643-1652.

Xiong, Y., A. Mahmood, and M. Chopp. 2013. Animal models of traumatic brain injury. *Nature reviews. Neuroscience*. 14:128-142.

Yi, J.H., and A.S. Hazell. 2005. N-acetylcysteine attenuates early induction of heme oxygenase-1 following traumatic brain injury. *Brain research*. 1033:13-19.

Yu, X., N. Song, X. Guo, H. Jiang, H. Zhang, and J. Xie. 2016. Differences in vulnerability of neurons and astrocytes to heme oxygenase-1 modulation: Implications for mitochondrial ferritin. *Scientific reports*. 6:24200.

Zhang, Z., Y. Song, Z. Zhang, D. Li, H. Zhu, R. Liang, Y. Gu, Y. Pang, J. Qi, H. Wu, and J. Wang. 2017. Distinct role of heme oxygenase-1 in early- and late-stage intracerebral hemorrhage in 12-month-old mice. *Journal of cerebral blood flow and metabolism : official journal of the International Society of Cerebral Blood Flow and Metabolism*. 37:25-38.

Zhang, Z., Z.Y. Zhang, Y. Wu, and H.J. Schluesener. 2012. Immunolocalization of Toll-like receptors 2 and 4 as well as their endogenous ligand, heat shock protein 70, in rat traumatic brain injury. *Neuroimmunomodulation*. 19:10-19.
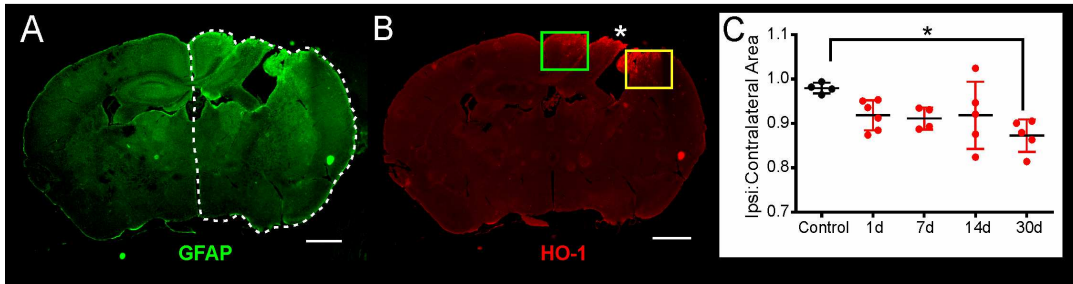
Figure 1. Regions of interest for cell counting and tissue loss after TBI.

(A) Lesion area (relative tissue loss) was demarcated on GFAP-stained tissue comparing ipsilateral hemispheres (dotted white line) and contralateral hemisphere as a ratio to determine lesion area following moderate TBI (see C). (B) Two perilesional cortical regions (boxes) adjacent to the lesion were analyzed for quantification of HO-1$^+$ microglia and astrocytes. Asterisk indicates site of injury. (C) Lesion area was quantified at each time point after injury. Despite tissue heterogeneity there was a sustained loss of tissue on the ipsilateral brain at 30dpi (* $p<0.01$). Scale bars = 1mm for A, B.
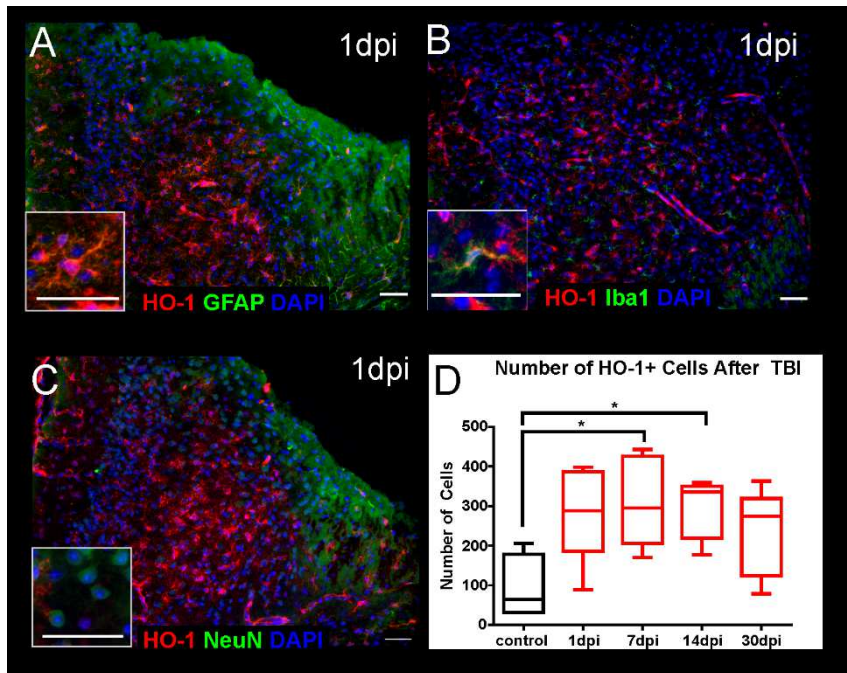
Figure 2. Cell types expressing HO-1 after TBI and temporal evolution of total HO-1$^+$ cells.

(A) Perilesional cortex at 1dpi adjacent to the lesion illustrating HO-1 and GFAP immunostaining where a subset of GFAP cells also express HO-1. (B) Iba1 and HO-1 immunostaining in the perilesional cortex at 1dpi were colocalized. (C) In contrast, there was a lack of neuronal (NeuN) and HO-1 colocalization in the perilesional cortex. (D) The number of HO-1$^+$ cells quantified over time (Control vs 7dpi *p<0.03, control vs 14dpi *p<0.03). Scale bars =50 μm for A-C.
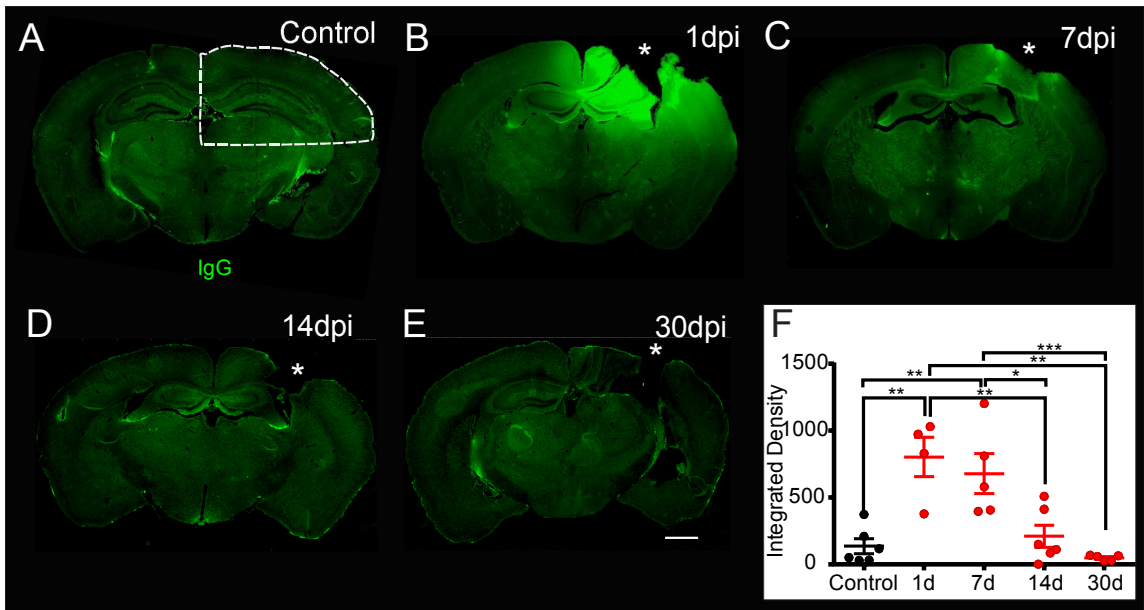
Figure 3. Blood-brain barrier integrity (BBB) after TBI.

(A) BBB integrity after TBI was assessed using IgG staining. Controls (shams) did not exhibit any IgG leakage. Outline (dotted line) illustrates the region used for quantification of BBB leakage following TBI. (B) IgG staining was dramatically increased in the ipsilateral cortex and hippocampus of mice 1dpi. (C) Moderate, but reduced IgG was still visible at 7dpi. (D) At 14dpi there was minimal IgG leakage evident in the majority of TBI mice. (E) BBB leakage at 30dpi was absent in the ipsilateral cortex. (F) Quantification (integrated densities, a.u.) of IgG staining at the injury site revealed significantly increased BBB disruption at 1-7dpi with return to control levels by 30dpi (control vs. 1dpi **p<0.001, control vs. 7dpi ** p<0.004, 1dpi vs. 14dpi **p<0.003, 1dpi vs. 30dpi ***p<0.004, 7dpi vs. 14dpi *p<0.02, 7dpi vs. 30dpi **p<0.001). Scale bar for all images = 1mm.
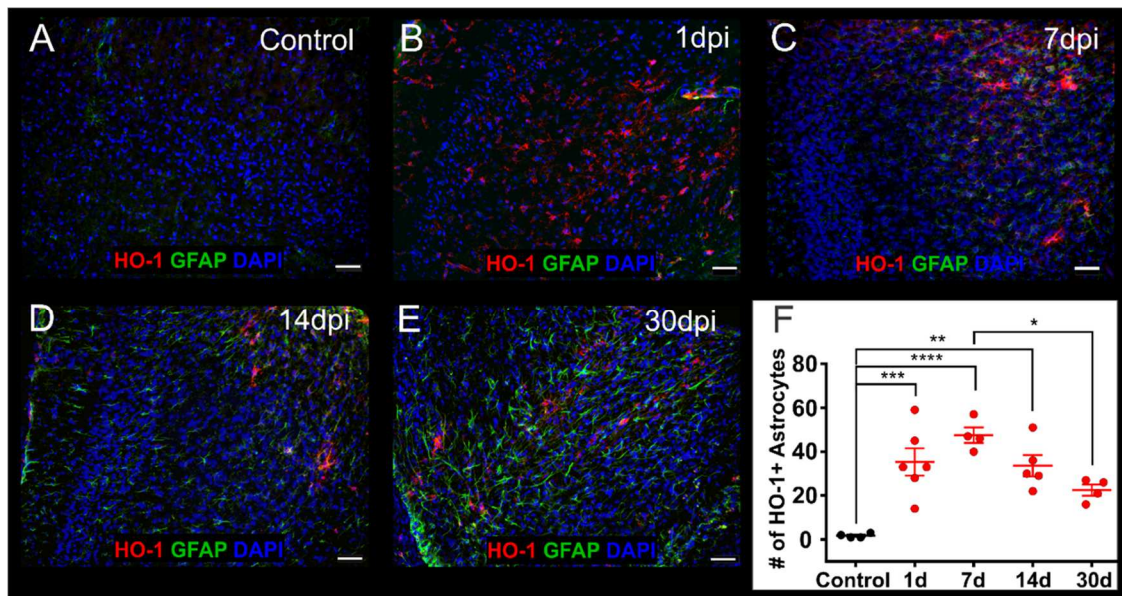
Figure 4. HO-1 expression in astrocytes following TBI.

HO-1 and GFAP colocalization in the ipsilateral cortex of control and injured mice adjacent to the lesion site (20X magnification) from control (A) and TBI mice at 1dpi (B), 7dpi, (C) 14dpi, (D) and (E) 30dpi. (F) Quantification of HO-1$^+$ GFAP astrocytes demonstrated increased colocalization that peaked at 7dpi and remained elevated to 30dpi relative to uninjured controls. Each data point represents the total number of colocalized cells for one animal (*: $p<0.004$, **: $p<0.001$, ***: $p<0.0002$). Scale bar = 50 μm.
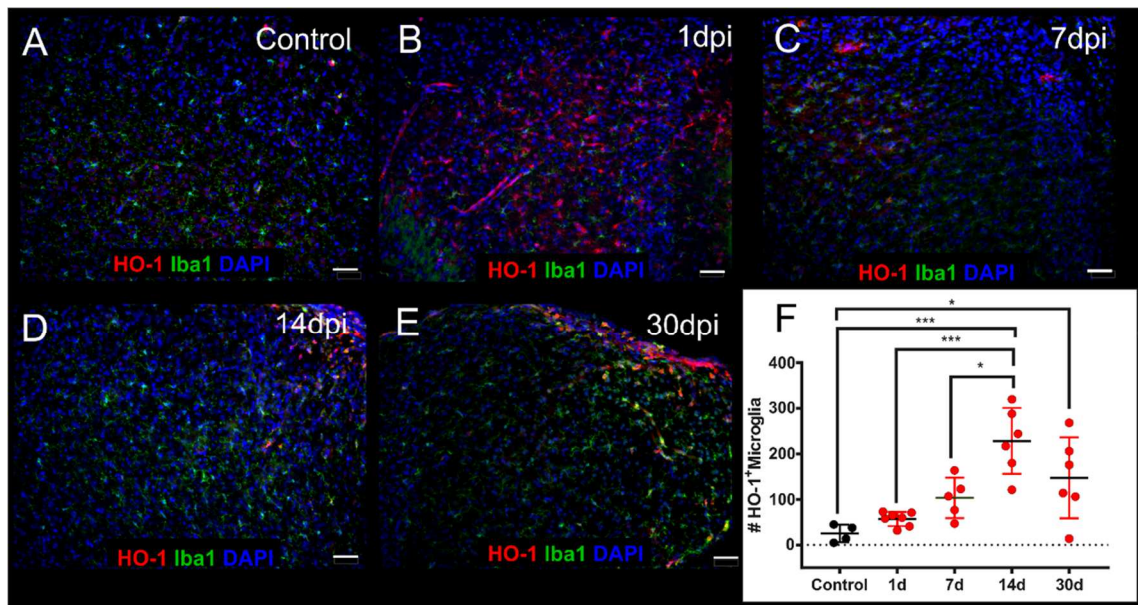
Figure 5. HO-1 expression in microglia following TBI.

Co-staining for HO-1 and Iba1 in the ipsilateral perilesional cortex of control and injured mice. Photomicrographs of perilesional cortex adjacent to the lesion in control (A), 1dpi (B), 7dpi (C), 14dpi, (D), 30dpi (E) mice following a moderate TBI. (F) Quantification of HO-1 and Iba1 colocalization identified that HO-1$^+$ microglia peaked at 14dpi and remained elevated at 30dpi. Note that the number of HO-1$^+$ microglia never return to control levels. Each data point represents the total number of colocalized cells for one animal (** $p<0.01$, *** $p<0.001$, **** $p<0.0001$). Scale bar = 50 μm.
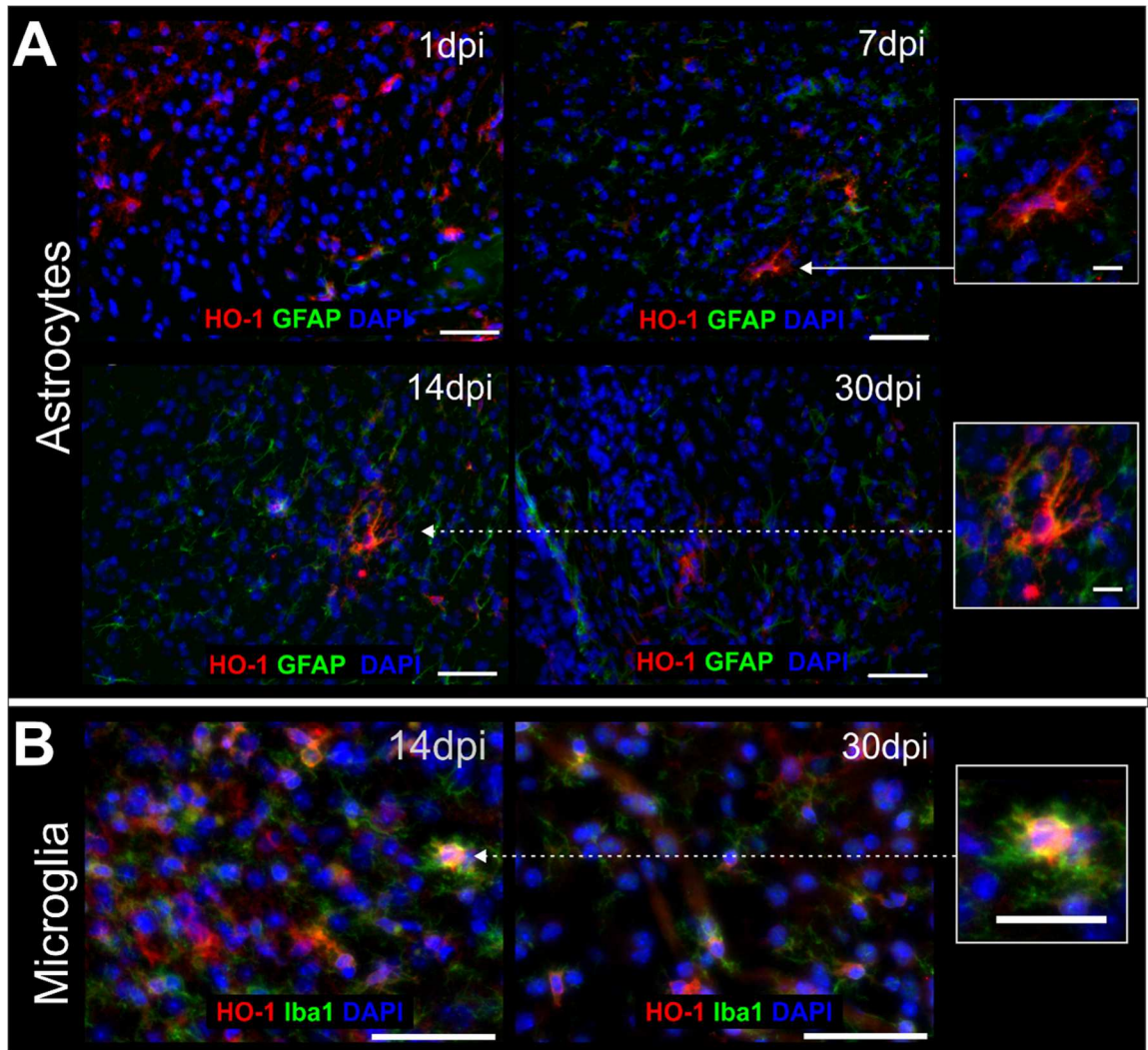
Figure 6. Morphologic comparisons of HO-1$^+$ expressing cells.

(A) Astrocytes expressing HO-1 appeared stellate in shape at 1dpi and by 7dpi appeared with a hypertrophied morphology including thickened processes (see inset to right). The astrocytic hypertrophic appearance was still evident at 14dpi (see inset to right) but by 30dpi astrocyte numbers were reduced and were more amoeboid in shape. (B) Microglia expressing HO-1 at 14dpi and 30dpi. A: 20x magnification. B: 40x magnification. S cale bar = 50 μm; inset scale bar = 25 μm.
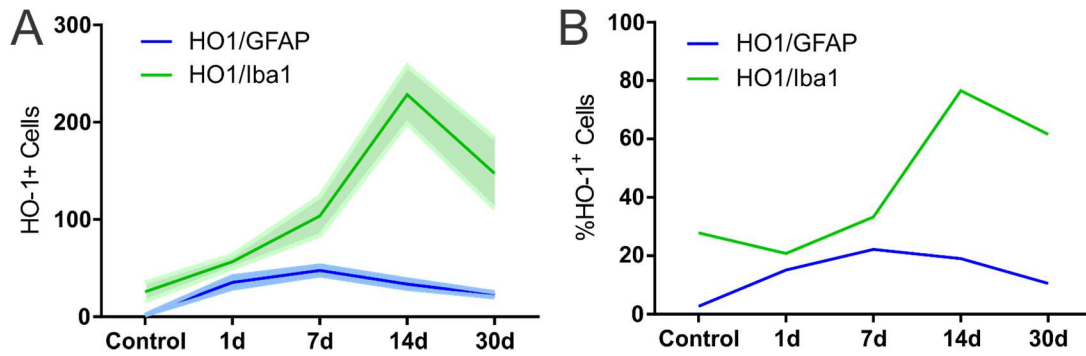
Figure 7. Temporal colocalization of HO-1 with glial cells and percentage contribution of HO-1$^+$ glial cells over total HO-1$^+$ cells.

(A) Average number of HO-1$^+$ astrocytes (solid blue line) and microglia (solid green line) in the injured cortex over time after moderate TBI, illustrating that HO-1$^+$ microglia peak at 14dpi. However, both astrocytes and microglia have a maintained level of co-expression within the perilesional cortex. Lighter shaded lines indicate S.E.M. (B) The percentage of GFAP$^+$ (solid blue line) and Iba1$^+$ cells expressing HO-1 over the total number of HO-1$^+$ cells over time after TBI.